JBC RESEARCH ARTICLE

An insulin-independent mechanism for transcriptional regulation of *Foxo1* in type 2 diabetic mice

Received for publication, January 27, 2021, and in revised form, May 8, 2021 Published, Papers in Press, May 28, 2021,
https://doi.org/10.1016/j.jbc.2021.100846

Wenhao Ge[‡], Yang Zhao[‡], Yunxia Yang, Zhao Ding, Xi Xu, Dan Weng, Shiming Wang, Rui Cheng[*], and Jianfa Zhang[*]

From the Center for Molecular Metabolism, Nanjing University of Science & Technology, Nanjing, China

Edited by Qi-Qun Tang

Hepatic gluconeogenesis is the major contributor to the hyperglycemia observed in both patients and animals with type 2 diabetes. The transcription factor FOXO1 plays a dominant role in stimulating hepatic gluconeogenesis. FOXO1 is mainly regulated by insulin under physiological conditions, but liver-specific disruption of *Foxo1* transcription restores normal gluconeogenesis in mice in which insulin signaling has been blocked, suggesting that additional regulatory mechanisms exist. Understanding the transcriptional regulation of *Foxo1* may be conducive to the development of insulin-independent strategies for the control of hepatic gluconeogenesis. Here, we found that elevated plasma levels of adenine nucleotide in type 2 diabetes are the major regulators of *Foxo1* transcription. We treated lean mice with 5′-AMP and examined their transcriptional profiles using RNA-seq. KEGG analysis revealed that the 5′-AMP treatment led to shifted profiles that were similar to *db/db* mice. Many of the upregulated genes were in pathways associated with the pathology of type 2 diabetes including *Foxo1* signaling. As observed in diabetic *db/db* mice, lean mice treated with 5′-AMP displayed enhanced *Foxo1* transcription, involving an increase in cellular adenosine levels and a decrease in the S-adenosylmethionine to S-adenosylhomocysteine ratio. This reduced methylation potential resulted in declining histone H3K9 methylation in the promoters of *Foxo1*, *G6Pc*, and *Pepck*. In mouse livers and cultured cells, 5′-AMP induced expression of more FOXO1 protein, which was found to be localized in the nucleus, where it could promote gluconeogenesis. Our results revealed that adenine nucleotide-driven *Foxo1* transcription is crucial for excessive glucose production in type 2 diabetic mice.

The liver plays a central role in whole-body homeostasis and metabolic health. Many metabolic functions, including lipid processing and distribution, amino acid synthesis, and gluconeogenesis, are performed or controlled by the liver (1). Hepatic gluconeogenesis is primarily responsible for the increase of fasting hepatic glucose production in individuals with type 2 diabetes (2). The transcription factor forkhead box protein O1 (FOXO1) plays a dominant role in regulating hepatic gluconeogenesis (3, 4). The FOXO1 interacts directly with DNA-binding sites in the promoter region of several genes related to gluconeogenesis (5, 6), stimulating glucose production in both mouse livers and isolated hepatocytes (4). The phosphorylation state of FOXO1 determines its cellular localization and transcription activity of FOXO1, which is mainly regulated by the insulin signaling pathway under physiological conditions (7). Insulin activates Akt to phosphorylate FOXO1 protein and causes a higher binding affinity of FOXO1 with chaperone protein, thus facilitating the cytoplasmic retention and nuclear export of FOXO1 (4, 8). Phosphorylated FOXO1 in the cytoplasm remains inactive and is finally degraded by the ubiquitin-proteasome pathway (8, 9).

Increased *Foxo1* transcription has been observed in the livers of *db/db* diabetic mice and patients with insulin resistance (10, 11). Deletion of hepatic *Foxo1* in diabetic mice improves insulin sensitivity and glucose tolerance (12, 13). Transgenic mice expressing the constitutively active *Foxo1* allele show an increase in gluconeogenesis and hepatic glucose production (14). *Foxo1* haploinsufficiency rescues diabetes in IRS2-deficient diabetic mice and prevents the development of high-fat diet-induced insulin resistance in wild-type (WT) mice (14, 15). Especially, disruption of *Foxo1* in a liver-specific manner restores glucose tolerance in insulin signal blocking mice (16, 17), implying suppression of *Foxo1* transcription may be an insulin-independent therapeutic approach for diabetes mellitus.

While insulin exerts its effects on gluconeogenesis in the liver by inactivating FOXO1 proteins (4), insulin has no effects on *Foxo1* transcription. The mechanism of hepatic *Foxo1* transcriptional regulation in type 2 diabetes mellitus is unknown. The factors that stimulate hepatic *Foxo1* transcription are generally considered to be less important than FOXO1 protein phosphorylation and are almost ignored in type 2 diabetes. Our previous observations demonstrate that the elevation of plasma adenine nucleotides is an upstream regulator in type 2 diabetic *db/db* mice (18, 19). An increasing amount of evidence highlights a critical role for the adenine nucleotides in the regulation of glucose homeostasis and the pathophysiology of diabetes mellitus (20). In the present study, we demonstrated that adenine nucleotides stimulate hepatic *Foxo1* transcription *via* suppressing histones methylation in

[‡] These authors contributed equally to this work.
[*] For correspondence: Jianfa Zhang, jfzhang@mail.njust.edu.cn; Rui Cheng, chengrui@njust.edu.cn.

type 2 diabetic *db/db* mice, indicating that adenine nucleotides-driven hepatic *Foxo1* transcription is crucial for excessive glucose production in type 2 diabetic mice.

Results

Adenine nucleotide activates Foxo signaling

To explore the unbiased biological association of the role of adenine nucleotides in diabetes, we used RNA sequencing to measure all poly A-containing transcripts in the livers of control and model mice. The significantly enriched pathways were identified by using the KEGG database. Mapping of annotated DEGs to KEGG pathways resulted in 249 DEGs of 42 pathways and 656 DEGs of 44 pathways in the livers of 5′-AMP-treated (Fig. 1*A*, upper) and *db/db* mice (lower), respectively (Supporting information S1–S4). Among these, a total of 42 KEGG pathways were disrupted simultaneously in both mouse models, indicating a high degree of similarity in gene transcription changes between the AMP group and the DB group. The 175 genes that are significantly changed in the AMP group overlapped with the same genes in the DB group (Fig. 1*B*, left). A heat map of the 175 genes with significant regulatory functions was constructed (Fig. 1*B*, right). Pearson r analysis showed that there was a strong correlation between biological repeats in each group. Next, we used ingenuity pathway analysis to identify the top 20 classic pathways implicated by gene expression changes, revealing many metabolic pathways, including glucagon signaling, insulin signaling, and insulin resistance, which showed consistent changes in the AMP and the DB group (Fig. 1*C*). Moreover, the Foxo signaling pathway was found to be one of the largest spots and was shown in the KEGG enrichment diagram of the AMP group (Fig. 1*D*), and the gluconeogenesis-related genes in the Foxo signaling pathway were activated (Fig. 1*E*). Similarly, the Foxo signaling pathway in the DB group has changed (Supporting Information S5). Although KEGG pathway analysis showed some changes between the AMP group and the DB group, there was no significant difference in the pathways related to type 2 diabetes (Fig. S1). Therefore, we speculate that 5′-AMP is likely to regulate hepatic gluconeogenesis through Foxo signaling.

Adenine nucleotide promotes hepatic gluconeogenesis

To verify the reliability of RNA-Sequencing data, eight responsive genes of 175 genes changed both in the AMP and the DB group were analyzed by qRT-PCR analysis. As shown in Figure 2*A*, the mRNA levels of *Mfsd2a*, *Slc25a25*, *Etnppl*, *Actg1*, *Klf3*, *Foxo1*, *G6Pc*, and *Pepck* were elevated in both groups. 5′-AMP significantly increased the transcription of gluconeogenesis-related genes including *Foxo1*, *G6Pc*, and *Pepck*, which were closely related to Foxo signaling and insulin resistance. Then, we investigated the function of 5′-AMP in regulating hepatic gluconeogenesis *in vivo*. 5′-AMP increased the glucose area under the curve during the pyruvate tolerance test (PTT) (Fig. 2*B*). PTT experiments confirmed that gluconeogenesis also increased in the *db/db* mice (Fig. 2*B*). Using different gluconeogenic substrates, we also found that 5′-AMP significantly increased glucose appearance with intraperitoneal (i.p.) administration of glycerol (Fig. 2*C*), lactate (Fig. 2*D*), fructose (Fig. 2*E*), and glutamine (Fig. 2*F*), respectively. The same results were obtained with *db/db* mice (Fig. 2, *C*–*F*). PTT experiments confirmed that 5′-AMP accelerated the consumption of gluconeogenic substrate pyruvate (Fig. 2*G*). Moreover, inhibition of FOXO1 function by selective FOXO1 inhibitor AS1842856 (21) eliminated 5′-AMP-induced hepatic gluconeogenesis during PTT (Fig. 2*H*). Together, these results indicate that 5′-AMP stimulates *Foxo1* transcription and promotes hepatic gluconeogenesis.

Adenine nucleotide stimulates hepatic Foxo1 *transcription*

To investigate the underlying mechanism of 5′-AMP-dependent hepatic gluconeogenesis, we first examined the effects of 5′-AMP on the expression levels of *Foxo1* mRNA and protein. 5′-AMP caused a dose-dependent increase in the mRNA levels of *Foxo1*, *Pepck*, and *G6Pc* in mouse livers (Fig. S2). Western blotting analysis showed that the FOXO1 protein level was also increased in 5′-AMP-treated livers (Fig. 3*A*). Moreover, 5′-AMP decreased the phosphorylation level of FOXO1 (Fig. 3*B*). Immunofluorescence analysis showed that the fluorescence intensity of FOXO1 was significantly increased after 5′-AMP, and the immunofluorescence of FOXO1 was mainly localized in the nucleus (Fig. 3*C*). These observations indicate that 5′-AMP enhances *Foxo1* transcription as well as FOXO1 nuclear translocation.

5′-AMP-stimulated Foxo1 *transcription is related to cellular methylation potential*

To clarify how 5′-AMP stimulates hepatic *Foxo1* transcription, a transcription inhibitor actinomycin D (AD) was used to explore the underlying mechanism. The results revealed that the AD significantly blocked the transcription level of *Foxo1* in the livers of 5′-AMP-treated mice and *db/db* mice, excluding the possibility of posttranscriptional regulation of *Foxo1* mRNA by 5′-AMP (Fig. 4, *A* and *B*), suggesting that 5′-AMP increased *Foxo1* mRNA level through a process involving *de novo* gene transcription. Because 5′-AMP can be dephosphorylated into adenosine by 5′-nucleotidase anchored on the cell membranes, the function of 5′-AMP may play a role *via* increasing intracellular adenosine levels or acting on specific cell surface receptors (21). Administration of adenosine also increased hepatic *Foxo1* transcription (Fig. 4*C*) and promoted gluconeogenesis in mice (Fig. 4*D*). To determine whether the effects of adenosine were due to the engagement of adenosine receptors, mice were treated with the broad-spectrum adenosine receptor antagonist theophylline. Theophylline treatment did not lower *Foxo1* mRNA levels seen in 5′-AMP mice (Fig. 4*E*). Next, we found that a methyl donor betaine reduced *Foxo1* mRNA in the livers of 5′-AMP-treated mice (Fig. 4*F*) and *db/db* mice (Fig. 4*G*). Cycloleucine acts as a competitive inhibitor of methionine S-adenosyl transferase involved in regulating the ratio of S-adenosylmethionine (SAM)/S-adenosylhomocysteine (SAH), the cellular methylation potential (22). The methylation inhibitor cycloleucine significantly

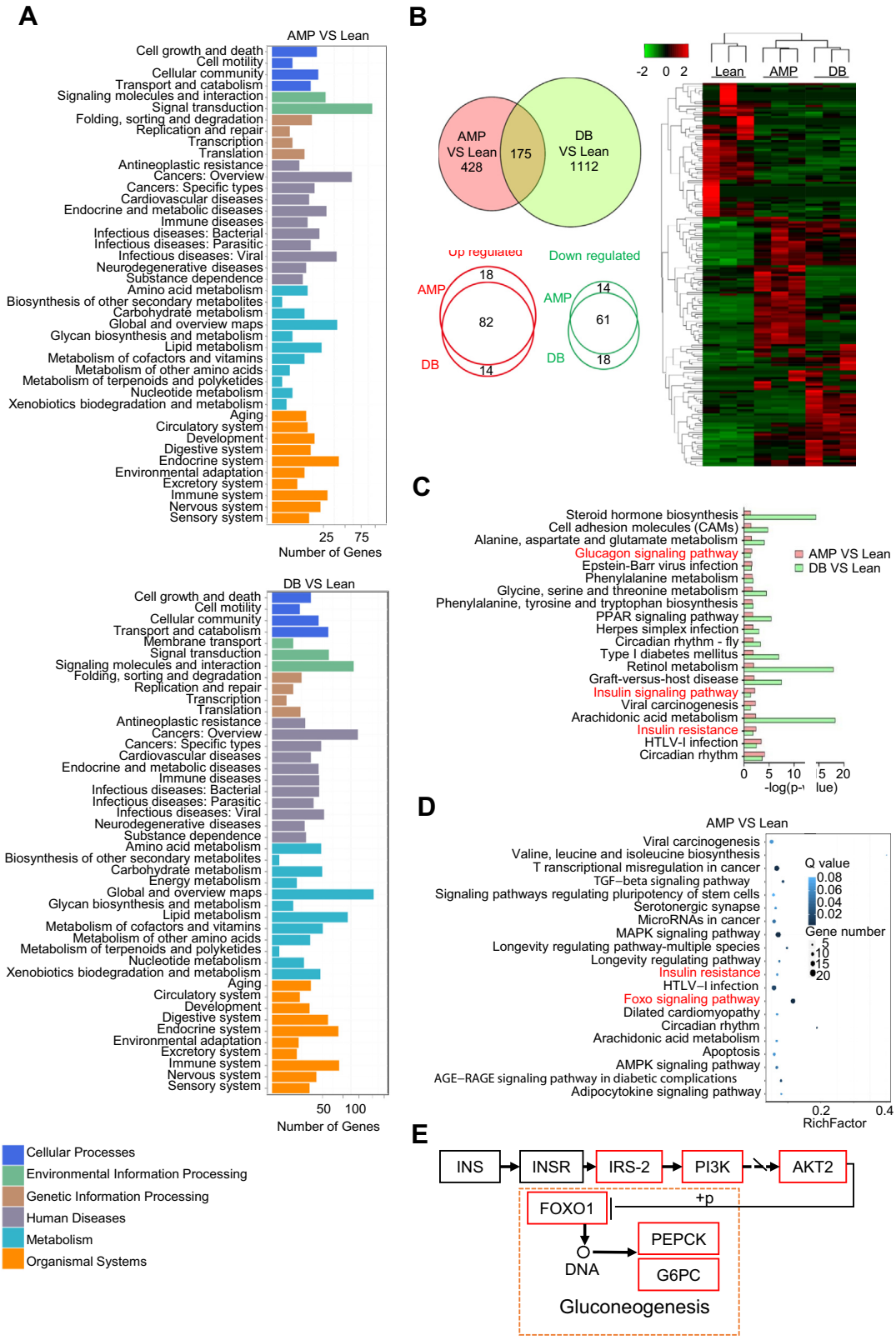

Figure 1. Global identification of mRNA expression in the livers from diabetic *db/db* and 5′-AMP-treated mice. *A*, distribution of the KEGG pathways at level 2 in the livers of the mice with 5′-AMP injection for 1 h (0.5 μmol/g i.p.), and diabetic *db/db* mice, respectively. The bar chart showed the numbers of sequences within different pathway categories. *B*, Venn diagram illustrating the extent of overlap among the differentially expressed genes observed in each group. The 175 genes regulated in the AMP group significantly overlapped with the same genes in the DB group. Venn diagram for upregulated genes or downregulated genes among 175 genes was shown. Heatmap representation of 175 overlapping genes was constructed. *C*, top 20 pathways altered in both 5′-AMP-treated mice and diabetic *db/db* mice. *D*, top 20 most significantly altered pathways at the AMP group. *E*, Foxo signaling pathway was activated in the AMP group. *Red* represented upregulation. n = 3 animals per group.

increased *Foxo1* mRNA levels in WT livers (Fig. 4*F*). HPLC analysis showed that betaine, but not theophylline, increased the ratio of SAM/SAH in the livers of 5′-AMP mice (Fig. 4, *H* and *I*) and *db/db* mice (Fig. 4*J*). As expected, cycloleucine significantly reduced the ratio of SAM to SAH in mouse livers (Fig. 4*I*). These results demonstrate that 5′-AMP-stimulated *Foxo1* transcription is closely related to cellular methylation potential. Then we examined whether 5′-AMP influences DNA methylation. As shown in Figure 4*K*, the DNA methylation levels of the *Foxo1* promoter remained unchanged in the livers of 5′-AMP-treated mice. Similar results were observed in that of *db/db* mice (Fig. 4*K*).

Adenine nucleotide decreases histone H3K9 methylation

Histone methylations are known to control gene expression (23). Increased histones methylation of some specific amino acid residues is generally associated with transcriptional silencing and heterochromatin formation, which ensures stable repression and genomic integrity (24). Then we detected a

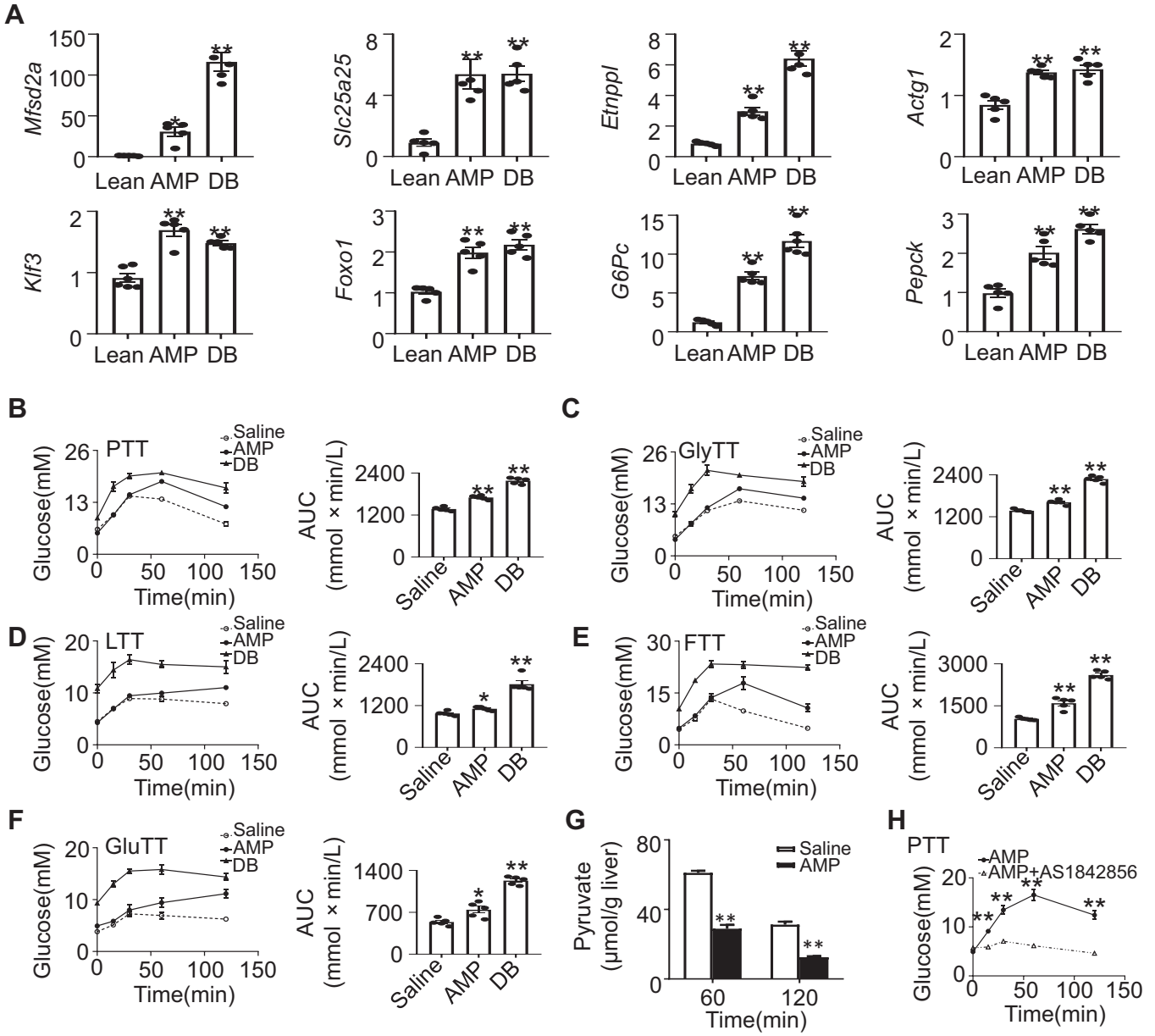

Figure 2. Increased hepatic glucose production in 5′-AMP-treat mice. *A*, quantitative real-time RT-PCR analysis confirmed an elevation of mRNA levels including *Mfsd2a*, *Slc25a25*, *Etnppl*, *Actg1*, *Klf3*, *FoxO1*, *G6Pc*, and *Pepck* in the livers of 5′-AMP-treated mice (0.5 μmol/g i.p.) and diabetic *db/db* mice. *B*, the tolerance tests were assessed in 5′-AMP-treated mice and diabetic *db/db* mice fasted for 16 h by intraperitoneally injection with pyruvate (2 g/kg), (*C*) glycerol (2 g/kg), (*D*) lactate (1.5 g/kg), (*E*) fructose (2 g/kg), and (*F*) glutamine (1.5 g/kg), respectively. Blood glucose levels were measured at indicated time points. Area under the blood glucose–time curve (AUC) was calculated. *G*, pyruvate concentrations in the liver were measured at 60 or 120 min in mice fasted for 16 h by intraperitoneal injection with pyruvate (2 g/kg). *H*, time course of changes in the plasma glucose levels during the pyruvate tolerance test in mice treated with AS1842856 (30 μg/g i.p.) and 5′-AMP (0.5 μmol/g i.p.). Data represent means ± SEM, n = 5 per group. *p value < 0.05, **p value < 0.01, compared with control group.

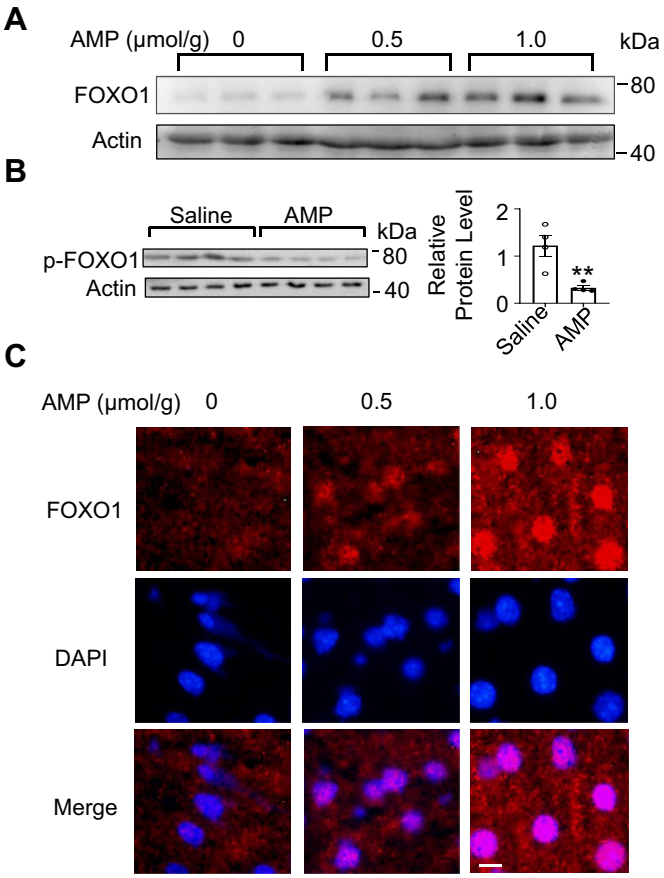

Figure 3. Activated hepatic *Foxo1* transcription and increased nuclear accumulation of FOXO1 in 5′-AMP-treated mice. *A*, hepatic protein levels of FOXO1 were analyzed by western blotting. β-actin was used as internal control. n = 3 animals per group. *B*, hepatic protein levels of p-FOXO1 were analyzed by western blotting. β-actin was used as internal control. Data represent means ± SEM, n = 4 animals per group. **p* value < 0.05, ***p* value < 0.01, compared with control mice. *C*, representative immunofluorescent appearance of the localization of endogenous FOXO1 in mice treated with 5′-AMP. The sections were counterstained with DAPI (*blue*) and immunostained for FOXO1 (*red*). Scale bar = 10 μm. The fluorescence staining indicated that 5′-AMP increased the nuclear accumulation of FOXO1.

significant reduction in total H3K9me2 methylation in the livers of 5′-AMP-treated mice (Fig. 5*A*). The observation of a reduction in methylation epitopes associated with transcriptional repression (H3K9) chromatin suggests that hypomethylation may occur at the genome-wide level. Then, chromatin immunoprecipitation (ChIP) analysis was performed to compare histone methylation levels in *Foxo1*, *G6Pc*, and *Pepck* promoter regions. Compared with the control group, 5′-AMP resulted in a significant decrease of H3K9me2 levels in the promoter regions of *Foxo1*, *G6Pc*, and *Pepck* (Fig. 5*B*). The results of the ChIP analysis were confirmed by ChIP-qPCR (Fig. 5*C*). We also detected a significant reduction in H3K9 methylation in *db/db* livers by western blotting analysis (Fig. 5*D*). ChIP assay and qPCR analysis demonstrated that the H3K9me2 levels, as observed in 5′-AMP-treated mice, were markedly decreased in the promoter regions of *Foxo1*, *G6Pc*, and *Pepck* in *db/db* mice (Fig. 5, *E* and *F*). Together, our results suggest that the overall decrease of H3K9me2, specifically the reduction of *Foxo1*, *G6Pc*, and *Pepck* promoter locus, results in transcriptional stimulation of these genes in 5′-AMP-treated and *db/db* mice.

Adenine nucleotide promotes Foxo1 *transcription in cultured cells*

To confirm the results we obtained from the mouse livers, we used HepG2 cells to investigate the effects of 5′-AMP on the regulation of *Foxo1 in vitro*. The results showed that 5′-AMP resulted in a significant increase of glucose production in HepG2 cells (Fig. S3). HPLC analysis revealed that 5′-AMP caused a significant decrease in the SAM/SAH ratio (Fig. 6*A*). Then, we investigated whether nonspecific adenosine receptor antagonist (theophylline) and adenosine transporter inhibitor (dipyridamole) affect cell methylation potential and are related to *Foxo1* transcription. As shown in Figure 6*A*, theophylline did not affect the 5′-AMP-decreased cellular methylation potential, and the adenosine transport inhibitor dipyridamole significantly inhibited the effect of 5′-AMP on methylation potential (Fig. 6*A*). To further explore the possible involvement of cellular methylation potential, we added SAM and the methylation inhibitor cycloleucine to observe the changes in the SAM/SAH ratio (Fig. 6*B*). The addition of SAM restored the 5′-AMP-decreased ratio of SAM/SAH. Twenty-four hours after the incubation of cycloleucine, the SAM/SAH ratio decreased significantly (Fig. 6*B*). The qRT-PCR analysis showed that 5′-AMP significantly increased *Foxo1* mRNA levels in HepG2 cells, and the addition of theophylline did not affect the regulation of *Foxo1* transcription by 5′-AMP (Fig. 6*C*). Notably, dipyridamole significantly decreased 5′-AMP-stimulated *Foxo1* transcription (Fig. 6*C*). In HepG2 cells, cycloleucine increased *Foxo1* transcription like 5′-AMP (Fig. 6*D*), and SAM eliminated the effects of 5′-AMP on *Foxo1* transcription regulation (Fig. 6*D*), further indicating that 5′-AMP regulates *Foxo1* transcription by affecting the methylation potential of cells. Immunofluorescence analysis was performed to show the subcellular location of FOXO1. While FOXO1 was mainly located in the cytoplasm in control cells, 5′-AMP significantly increased FOXO1accumulation in the nucleus (Fig. 6*E*). The theophylline did not affect 5′-AMP-regulated FOXO1 nuclear accumulation, but dipyridamole inhibited the appearances of FOXO1 in the nucleus. Moreover, SAM increased the intracellular cytoplasmic FOXO1 protein level and reduced the nuclear FOXO1 accumulation. Contrarily, cycloleucine markedly increased the appearances of FOXO1 in the nucleus (Fig. 6*E*).

Discussion

Hepatic *Foxo1* transcription is activated in the livers of patients with insulin resistance and type 2 diabetic mice (10, 11), playing a crucial role in excessive glucose production (25). The molecular mechanism that stimulates hepatic *Foxo1* transcription in type 2 diabetes is unknown and almost ignored. In the present study, we showed that 5′-AMP increased FOXO1 accumulation in the nucleus both *in vivo* and *in vitro*, thus promoting gluconeogenesis. This characterization was initially based on the induction of *Foxo1* at the transcription level, for

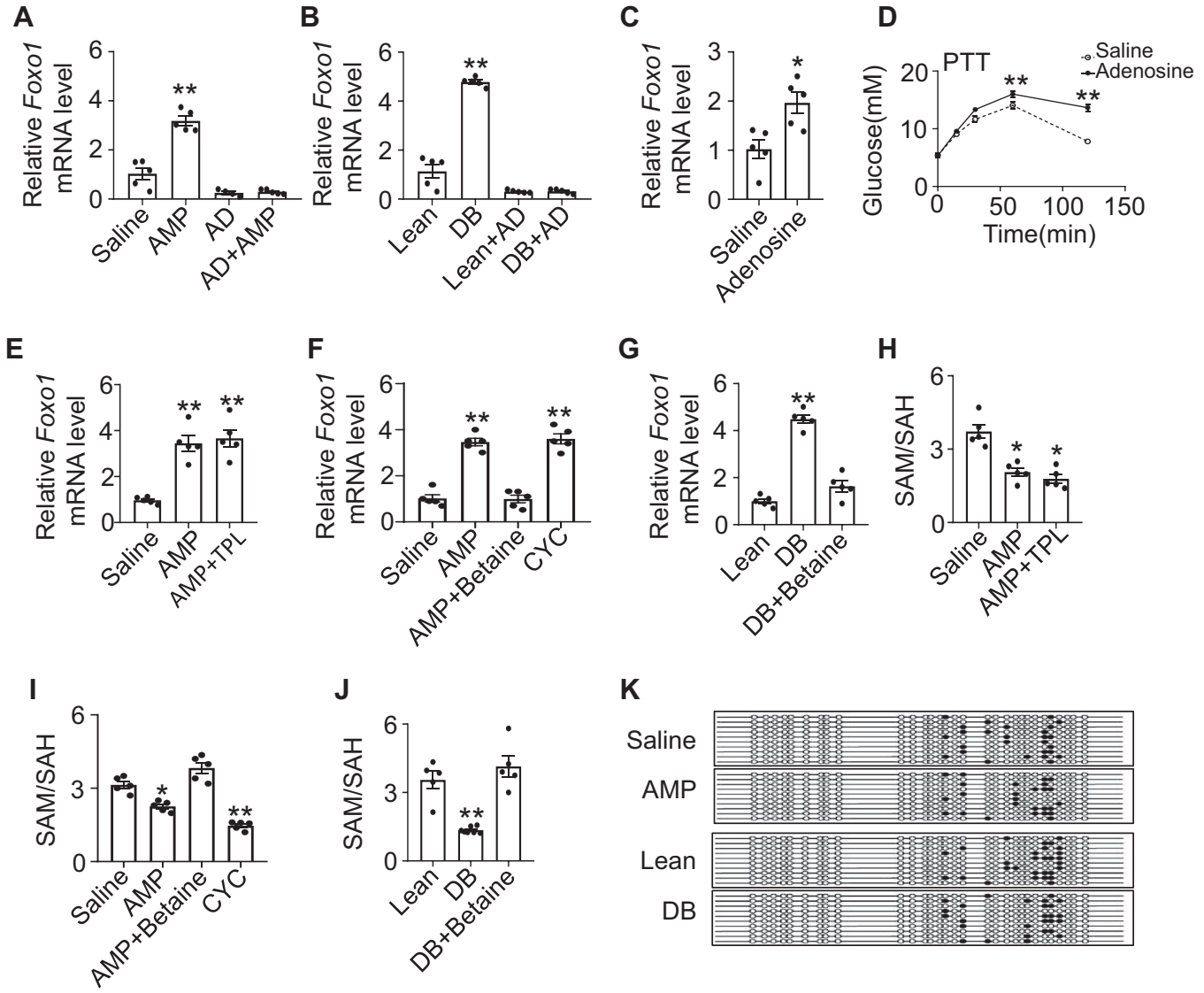

Figure 4. 5′-AMP-stimulated *Foxo1* transcription correlates with cell methylation potential. *A*, quantitate RT-PCR analysis of *Foxo1* mRNA of livers in mice treated with actinomycin D (AD, 3 nmol/g i.p.) and 5′-AMP (0.5 μmol/g i.p.); mice injected with AD during 60 min prior to 5′-AMP. Saline serves as control. *B*, quantitate RT-PCR analysis of *Foxo1* mRNA of livers in *db/db* mice treated with AD (3 nmol/g i.p.). *C*, quantitate RT-PCR analysis of *Foxo1* mRNA of livers in mice treated with adenosine (0.2 μmol/g i.p.). *D*, the pyruvate tolerance tests were assessed in adenosine-treated mice fasted for 16 h by intraperitoneal injection with pyruvate (2 g/kg). *E*, quantitate RT-PCR analysis of *Foxo1* mRNA of livers in mice treated with theophylline and 5′-AMP. AMP: 5′-AMP, i.p. 0.5 μmol/g; TPL: theophylline, i.p. 10 μg/g. Saline serves as control. *F*, quantitate RT-PCR analysis of *Foxo1* mRNA of livers in mice treated with betaine, cycloleucine, and 5′-AMP. AMP: 5′-AMP, i.p. 0.5 μmol/g; Betaine: betaine (2 mg/ml) in drinking water for 2 weeks prior to 5′-AMP injection; CLC: cycloleucine, i.p. 16 μmol/g. Saline serves as control. *G*, quantitate RT-PCR analysis of *Foxo1* mRNA of livers in *db/db* mice treated with methylation activator betaine. The betaine (2 mg/ml) was administrated in drinking water for 2 weeks. *H*, HPLC analysis of liver SAM and SAH in mice treated with theophylline and 5′-AMP. AMP: 5′-AMP, i.p. 0.5 μmol/g; TPL: theophylline, i.p. 10 μg/g. Saline serves as control. *I*, HPLC analysis of liver SAM and SAH in betaine and cycloleucine-treated mice. AMP: 5′-AMP, i.p. 0.5 μmol/g; Betaine: 2 mg/ml, in drinking water for 2 weeks prior to 5′-AMP; CLC: cycloleucine, i.p. 16 μmol/g. Saline serves as control. *J*, HPLC analysis of liver SAM and SAH in betaine-treated *db/db* mice, betaine (2 mg/ml) in drinking water for 2 weeks (n = 5, *A–J*). *K*, measurement of DNA methyl-cytosine in the *Foxo1* promoter region of 5′-AMP-treated (*upper*) and *db/db* (*lower*) livers. Saline and lean mice serve as controls, respectively. No significant changes in both group comparisons (n = 10). Data represent means ± SEM. **p* value < 0.05, ***p* value < 0.01, compared with control group.

the first time revealing that adenine nucleotides-driven *Foxo1* transcription is essential for excess glucose production in type 2 diabetes.

Free fatty acid (FFA) is an important link between obesity, insulin resistance, and type 2 diabetes (26). FFAs induce adenine nucleotides release from human umbilical vein endothelial cells (18, 27) and impair the resistance of red blood cells to reactive oxygen species, leading to hemolysis, thereby increasing plasma adenine nucleotides (27). Plasma-membrane-bound enzymes CD73 metabolize adenine nucleotides to adenosine (28). Adenosine works by activating G-protein-coupled adenosine receptors A_1, A_{2A}, A_{2B}, and A_3 (29). Under physiological conditions, A_{2A} adenosine receptors have been thought to play a role in modulating the function of FOXO1 (30). In our observations, adenosine transport inhibitor, but not adenosine receptor antagonist, significantly reduced 5′-AMP-stimulated *Foxo1* transcription. Adenosine also has its direct biochemical function, which is not directly

related to the adenosine receptor pathway (18, 31). The equilibrative nucleoside transporters passively transport adenosine across cell membranes by promoting diffusion (32). Under the pathological state of type 2 diabetes, the sustained high concentration of adenosine may passivate the regulatory effect of adenosine receptors. Our results suggest that 5′-AMP-stimulated *Foxo1* transcription is related to the transports rather than cell surface receptors.

Exogenous 5′-AMP results in a dose-dependent elevation in adenosine levels in the liver, thereby increasing SAH and decreasing SAM/SAH ratio (33). Our data showed that 5′-AMP promoted hepatic gluconeogenesis and increased glucose output, which was mediated by the methylation ability associated with the SAM/SAH ratio. SAH is a powerful inhibitor of all methylation reactions. The concentrations of SAM and SAH are associated with diabetes (34, 35). In patients with diabetes, especially in patients with kidney disease, the concentration of SAM and related compounds in blood changes abnormally (34). Compared with nondiabetic patients, the concentration of SAH in plasma and erythrocytes of patients with type 2 diabetes is also significantly higher (36). Antidiabetic drug metformin has been found to improve the methylation ability through the regulation of the SAM/SAH ratio (37), and insulin-regulating mTOR signaling is capable of changing DNA methylation.

The SAM/SAH ratio does not directly affect the daily changes in global DNA methylation (33). In our observation, the adenosine-driven SAM/SAH ratio did not change the DNA methylation level of the *Foxo1* gene, but it resulted in insufficient histone methylation associated with the *Foxo1* promoter region. Methylation of H3K9 is very common in transcriptional silencing (38), and H3K9 methylation is an inactive chromatin marker (39).

Therefore, the insufficient methylation of histone H3K9 in the *Foxo1* promoter region led to the activation of *Foxo1* gene transcription. In addition, the change of SAM/SAH ratio implied that hypomethylation may occur at the whole genome level. Thus, other genes related to diabetes pathways are probably also involved. In fact, we found that *Mfsd2a*, *Slc25a25*, *Etnppl*, *Actg1*, and *Klf3* were indeed elevated in both the AMP and the DB groups. Our analysis suggests a far more substantial role for adenine nucleotides in diabetes development.

Our previous observation showed that plasma 5′-AMP was elevated in type 2 diabetic *db/db* mice, and exogenous 5′-AMP caused type 2 diabetes-like hyperglycemia in lean mice (18). Plasma 5′-AMP was also elevated in patients with type 2 diabetes (19). Since adenosine was a potential inhibitor of insulin receptor (IR) tyrosine kinase, insulin-stimulated IR autophosphorylation was significantly attenuated by 5′-AMP treatment, resulting in a reduction of insulin sensitivity (40). We also provide evidence for adenine nucleotides regulating the activity of PTP1B in type 2 diabetic mice (19). Together, it strongly suggests that

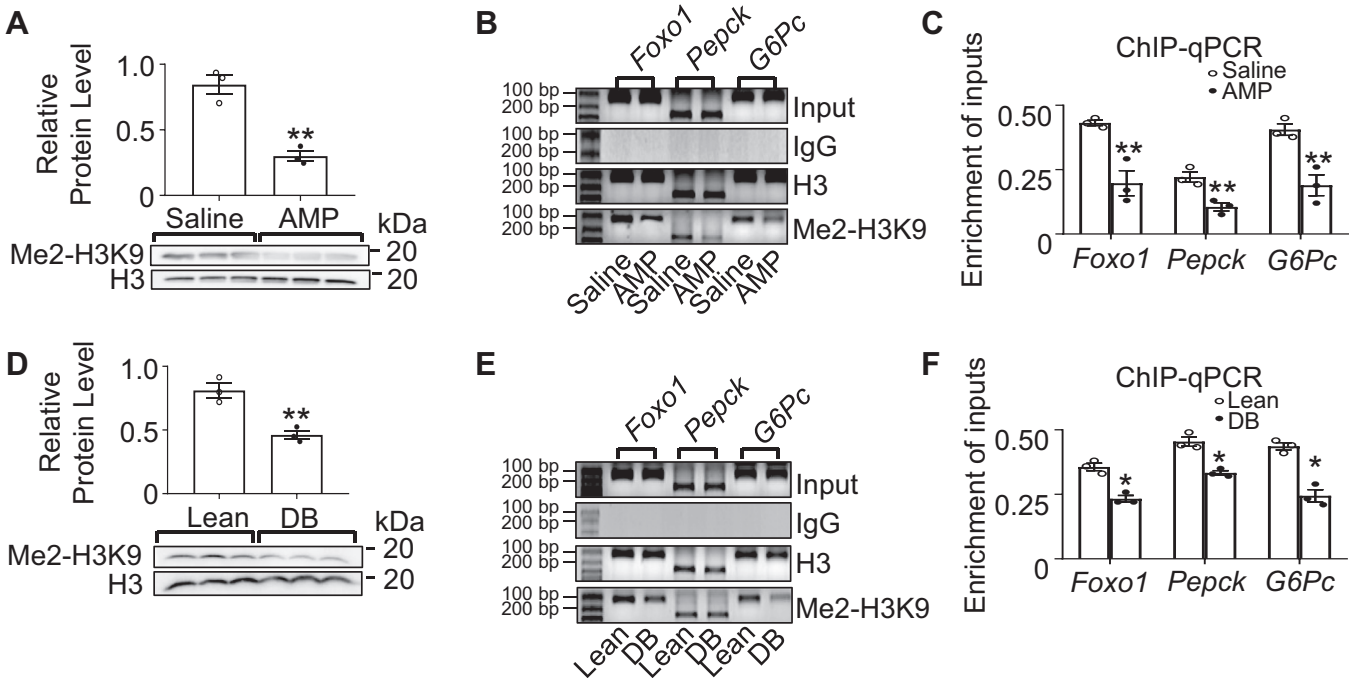

Figure 5. Reduced histone H3K9 methylation on *Foxo1* promoter by 5′-AMP. *A*, western blotting showing that methylated H3K9 was reduced in 5′-AMP-treated liver. H3 was used as internal control (n = 3). *B*, ChIP analysis using antibody against Di-Methyl-Histone H3 Lys9 (Me2-H3K9), followed by PCR with primers amplifying the *Foxo1*, *Pepck*, and *G6Pc*. Input, IgG control, and H3 serve as controls. The representative images showing that the methylation level of H3K9 at *Foxo1*, *Pepck*, and *G6Pc* promoter region was decreased after 5′-AMP. *C*, quantitative RT-PCR analysis of enrichment in H3K9me2 for Input- and ChIP-DNA samples (n = 3). *D*, western blotting analysis of methylated H3K9 in liver tissue obtained from *db/db* mice and control mice (n = 3). H3 was used as internal control. *E*, ChIP assay of H3K9 methylation at *Foxo1*, *Pepck*, and *G6Pc* promoter regions in *db/db* mice. The representative images showing that the methylation level of H3K9 in liver tissue was decreased in *db/db* mice. *F*, quantification of the enrichment in H3K9me2 with qRT-PCR analysis. Input- and ChIP-DNA samples were quantified using primers for the promoters of the *Foxo1*, *Pepck*, and *G6Pc* genes (n = 3). Data represent means ± SEM. **p* value < 0.05, ***p* value < 0.01, compared with control group.

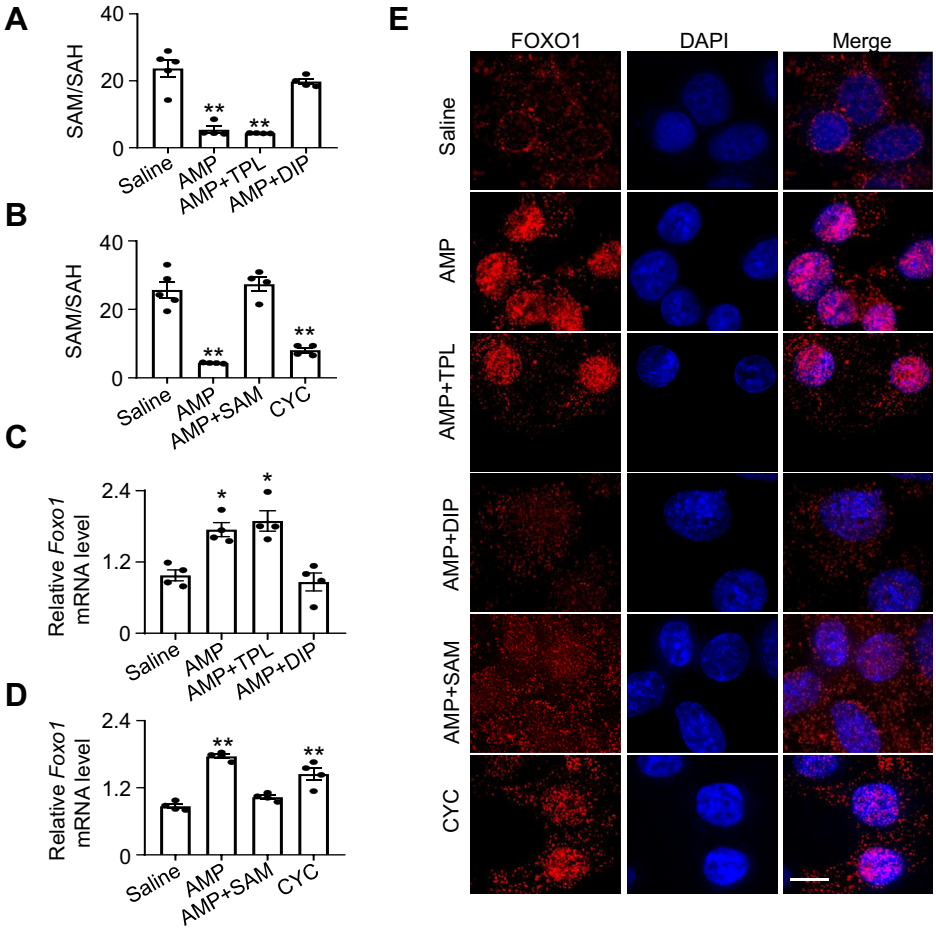

Figure 6. 5′-AMP promotes *Foxo1* transcription *in vitro*. *A*, HPLC analysis of SAM and SAH in HepG2 cells treated with adenosine receptor inhibitor theophylline (TPL, 100 μM), transporter blocker dipyridamole (DIP, 0.1 μM) plus 5′-AMP (AMP, 0.5 mM) for 24 h, respectively. n = 3. *B*, HPLC analysis of SAM and SAH in HepG2 cells treated with methylation inhibitor cycloleucine (CYC, 20 mM), methylation activator S-adenosylmethionine (SAM, 2 mM) and 5′-AMP (AMP, 0.5 mM) for 24 h. n = 3. *C*, quantitate RT-PCR analysis of *Foxo1* mRNA in HepG2 cells treated with TPL (100 μM), DIP (0.1 μM) plus AMP (0.5 mM) for 24 h, respectively. n = 3. *D*, quantitate RT-PCR analysis of *Foxo1* mRNA in HepG2 cells treated with CYC (20 mM), SAM (2 mM), and AMP (0.5 mM) for 24 h. n = 3. Data represent means ± SEM of n = 4 per group. **p* value < 0.05, ***p* value < 0.01, compared with control group. *E*, representative fluorescence images showing that subcellular 5′-AMP increases FOXO1 nucleus accumulation in HepG2 cells. The FOXO1 was visualized by immunofluorescence with specific antibodies (*red*). Nuclei were stained with DAPI (*blue*). Scale bar = 10 μm. Results were representative of at least three experimental replicates.

adenine nucleotides and insulins may antagonize each other on blood glucose homeostasis.

In conclusion, we revealed a novel molecular mechanism underlying that adenine nucleotides regulate *Foxo1* transcription for excessive glucose production in type 2 diabetes (Fig. 7). The mechanism of stimulating *Foxo1* transcription in type 2 diabetes is almost ignored. Our findings extend the current understanding of epigenetic regulation of hepatic gluconeogenesis through *Foxo1*, highlight the crucial role of adenine nucleotides in the development of type 2 diabetes, and reveal a novel strategy for diabetes treatment.

Experimental procedures

Mice

Eight-week-old male C57BL/6, C57BL/Ks *db/db* mice, and their lean littermates (+/+) were used in this study. Mice were housed in a standard animal facility under a 12-h/12-h light/dark cycle with free access to food and water. All procedures were approved by the Animal Care and Use Committee at Nanjing University of Science and Technology (ACUC-NUST-20170223).

Treatment of 5′-AMP, betaine, cycloleucine, and actinomycin D

5′-AMP (adenosine 5′-monophosphate disodium salt) was solvated in saline and administered to mice by intraperitoneal injection in doses of 0.5 or 1 μmol/g body weight at zeitgeber time (ZT)1. Adenosine was solvated in saline and administered to mice by intraperitoneal injection in doses of 0.2 μmol/g body weight at ZT1. Saline was injected as a control. To change cellular methylation potential, betaine was supplemented in the drinking water at a concentration of 2% (wt/vol) for 2 weeks before the test (41). To decrease SAM levels, cycloleucine was administered intraperitoneally (16 μmol/g body weight) at ZT1 (42). To inhibit mRNA transcription, actinomycin D was intraperitoneally (3 nmol/g body weight) injected into C57BL/6, C57BL/Ks *db/db* mice, and their lean littermates at ZT0. The transcriptional inhibitor actinomycin D was administered 60 min before the administration of 5′-AMP. To explore the role of adenosine receptors, adenosine

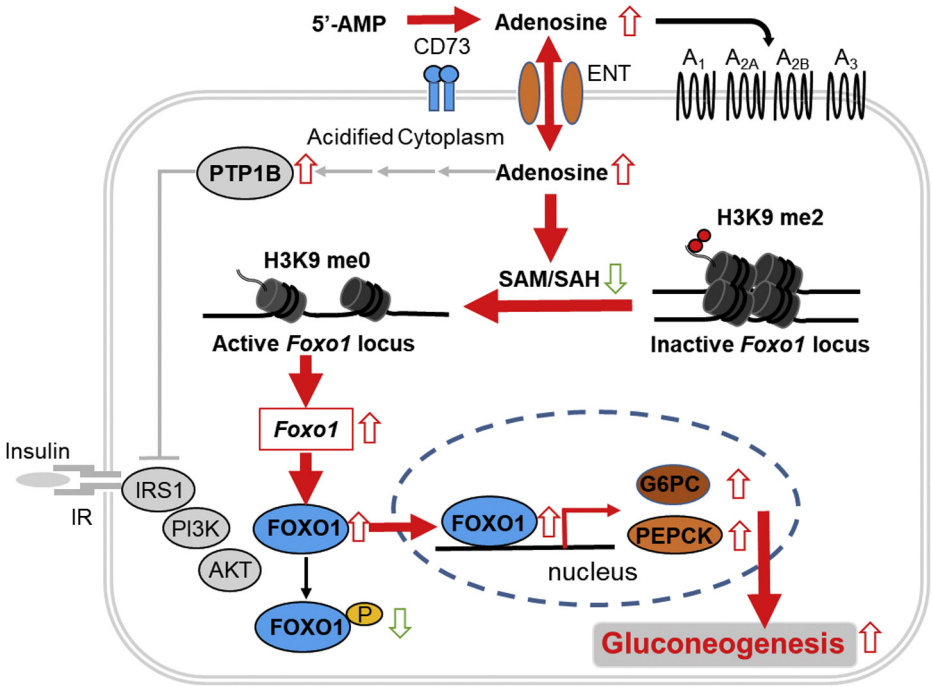

Figure 7. Schematic representation of the proposed regulatory function of 5′-AMP on modulating *Foxo1* transcription. Model showing that adenine nucleotides cause insufficient methylation of histone in the *Foxo1* promoter region, thereby activating *Foxo1* transcription.

receptor antagonist theophylline (10 μg/g, i.p.) was used 30 min before the administration of 5′-AMP. To inhibit FOXO1, mice were treated with AS1842856 (30 μg/g, i.p.) or the carrier solution 60 min before the administration of 5′-AMP. One hour after the injection of 5′-AMP, adenosine, or cycloleucine, all mice were sacrificed by cervical dislocation, and the livers were removed and freeze-clamped in liquid nitrogen for further analysis. Blood samples were immediately centrifuged at 5000 g for 5 min at 20 °C. The obtained plasma was immediately used. 5′-AMP, betaine, cycloleucine, theophylline, adenosine, and actinomycin D were from Sigma. AS1842856 was from MCE (HY-100596, MCE, China).

Gluconeogenesis tests

Gluconeogenesis tests were performed as described previously (43, 44). Briefly, mice were fasted overnight (16 h) prior to injected i.p. with pyruvate (2 g/kg BW), glycerol (2 g/kg BW), lactate (1.5 g/kg BW), fructose (2 g/kg BW), or glutamine (1.5 g/kg BW), respectively. 5′-AMP (0.5 μmol/g i.p.) or adenosine (0.2 μmol/g i.p.) was mixed with gluconeogenic substrates and coinjected into mice. Blood glucose levels were determined from the tail vein at 0, 15, 30, 60, and 120 min after injection, with a One Touch Ultra Blood Glucose Meter (Lifescan).

Measurement of pyruvate concentration

Hepatic pyruvate concentration was assayed with commercial kits according to the manufacturers' instructions (Jiancheng). Livers were homogenized in ice-cold PBS. Then, the homogenates were collected for pyruvic acid determination. Pyruvate concentration was normalized to the protein concentration of the samples.

RNA sequencing and analysis

Purified total RNA from the livers of 5′-AMP-treated, *db/db*, and control mice was used for RNA-sequencing preparation. cDNA library construction and sequencing were performed by Beijing Genomics Institute using a BGISEQ-500 sequencer. High-quality reads were aligned to the mouse genome (mm10) by using Bowtie2. The expression levels for each of the genes were normalized to fragments per kilobase of exon model per million mapped reads (FPKM) using RNA-seq by Expectation Maximization (RSEM).

Promoter methylation analysis

Quantitative DNA promoter methylation of *Foxo1* was performed by bisulfite sequencing PCR (BSP) (45). The primer sequences were shown in Table S1. Amplified DNA was ligated into the pCR2.1 vector (Invitrogen) and transformed into competent *E. coli* DH5α. Ten clones per sample were selected and sequenced. The results were analyzed by Biq Analyzer software.

HPLC analysis of SAM and SAH

SAM and SAH were extracted from frozen liver samples or PBS washed cell monolayers using 0.4 N perchloric acid (19, 46). SAM and SAH were measured by a reverse-phase HPLC (Waters 1525 system; Millipore Corp), according to the procedure previously described (33). The mobile phase contained 0.1 M sodium acetate, 5 mM heptanesulfonic acid adjusted to pH 4.5 with acetic acid, and 5.5% acetonitrile. The samples were eluted on a reversed-phase C18 column at room temperature with an invariable gradient at a flow rate of 0.8 ml/min. Characteristic peak spectra and retention times compared

with those of the standards were used to identify SAM and SAH. Quantitation was based on peak areas. SAM was from Solarbio. SAH was from Sigma.

RNA extraction and quantitative real-time PCR

Total RNA was extracted from livers and cells with Karrol reagent (Karroten Scientific) according to the manufacturer's instructions. Reverse transcript reaction was carried out by reverse transcript kit (Invitrogen) according to the manufacturer's protocol. Real-time PCR was performed with the SYBR Green PCR Kit (Applied Biosystems) following the manufacturer's instructions on an ABI 7300 real-time PCR system (Applied Biosystems) in a 20-μl volume. The relative mRNA levels of *Foxo1*, *Pepck*, and *G6Pc* were quantified, with *β-Actin* used for normalization. The primer sequences used for quantitative RT-PCRs were shown in Table S2.

Western blot analysis

Fresh livers and cells were homogenized, and proteins were extracted with an Extraction Reagent (KeyGEN) according to the manufacturer's instructions. The extraction was separated by SDS-PAGE 10%–15% polyacrylamide gel. The membranes were incubated with primary antibodies anti-FOXO1, phospho-FOXO1 (Ser-256), anti-Histone H3, and anti-Di-Methyl-Histone H3 Lys9 (Cell Signaling), respectively, following by incubation with HRP-conjugated secondary antibody (Boster) and detection by enhanced chemical luminescence kit (Thermo scientific). β-actin was used as a control.

Chromatin immunoprecipitation assays

ChIP assays were performed as described previously (47, 48). Cross-linked chromatin was immunoprecipitated with 5 μg of anti-Histone H3, anti-Di-Methyl-Histone H3 Lys9, respectively, or negative control rabbit IgG. Immunoprecipitated DNA was then used as a template for PCR. The primer sequences used for PCR were listed in Table S3.

Immunofluorescence analysis

Immunofluorescence and confocal microscopy were performed as described previously (49). Briefly, liver tissues were immersed in cryo-embedding medium and then sectioned into 10-μm-thick slices using a cryotome (Leica Microsystems). The cultured cells were washed three times with fresh PBS, fixed with 4% paraformaldehyde for 15 min, permeabilized with 0.25% Triton X-100 (Sigma) for 10 min. Slices and fixed cells were incubated with primary antibodies (anti-FOXO1, Cell Signaling) and secondary antibodies step by step. Nuclei were stained with DAPI. Fluorescence images of liver slices were observed with fluorescence microscopy (Eclipse 800; Nikon). The fluorescence images of cultured cells were acquired on a superresolution DeltaVision OMX imaging system (GE Healthcare).

HepG2 cells

HepG2 cells were maintained in Dulbecco's modified Eagle's medium (Gibco) supplemented with 10% fetal bovine serum (Gibco) and penicillin/streptomycin (10 μl/ml of medium, Gibco) at 37 °C in 5% (v/v) CO_2. To investigate the mechanisms responsible for the adenosine-mediated effects, the medium was removed and replaced with fresh medium, containing various concentrations of the compounds to be tested, for another 24 h: nontreated, 5′-AMP (0.5 mM) alone, 5′-AMP (0.5 mM) plus theophylline (100 μM), or dipyridamole (0.1 μM). To further confirm the regulatory effect of cell methylation potential, cells were treated with 5′-AMP for 24 h with or without 2 mM SAM. To inhibit methylation, cells were treated with 20 mM cycloleucine for 24 h. Theophylline, dipyridamole, SAM, and cycloleucine were purchased from Sigma.

Glucose production in cells

A previously established protocol was followed to estimate glucose production (50). HepG2 was plated in 6-well plates in 5% CO_2 incubator at 37 °C for 24–48 h. After 70–80% confluency cells were incubated overnight in DMEM media containing 2% charcoal-treated FBS and 1% antibiotics. Cells were washed three times with PBS to remove all traces of glucose and incubated with media containing 2% charcoal-treated FBS, phenol red, and glucose-free media for 2 h. Cells were treated with 0.5 mM 5′-AMP in glucose production assay medium (phenol red and glucose-free DMEM) containing 2 mM sodium pyruvate and 20 mM sodium lactate, pH 7.4, and incubated up to 24 h. A quantity of 300 μl of the medium was sampled for measurement of glucose concentration using a glucose assay kit (GAGO20, Sigma). Glucose values were normalized with cellular total protein concentrations.

Statistical analysis

The results were presented as means ± SEM. Statistical difference between groups was determined by Student's *t* test, and comparisons among groups were performed using ANOVA. A *p*-value of less than 0.05 indicated statistical significance.

Data availability

All data of this study are available in this article and in the supporting information. All source data generated for this study and relevant information are available from the corresponding author.

Supporting information—This article contains supporting information.

Acknowledgments—This work was supported by the grant from the National Natural Science Foundation of China (numbers 31871178, 31861163004).

Author contributions—W. G., R. C., and J. Z. conceptualization; J. Z. funding acquisition; W. G., Y. Z., and R. C. investigation; Y. Z., Y. Y, Z. D., and X. X. methodology; J. Z. project administration; Y. Y., Z. D., X. X., and R. C. resources; J. Z. supervision; Y. Z., Y. Y., Z. D., X. X., D. W., S. W., and R. C. validation; W. G., R. C., and J. Z. writing-

original draft; W. G., D. W., S. W., R. C., and J. Z. writing-review and editing.

Conflict of interest—The authors declare that they have no conflicts of interest with the contents of this article.

Abbreviations—The abbreviations used are: AD, actinomycin D; FFA, free fatty acid; FOXO1, forkhead box protein O1; PTT, pyruvate tolerance test; SAH, S-adenosylhomocysteine; SAM, S-adenosylmethionine.

References

1. Rhoads, T. W., Burhans, M. S., Chen, V. B., Hutchins, P. D., Rush, M. J. P., Clark, J. P., Stark, J. L., McIlwain, S. J., Eghbalnia, H. R., Pavelec, D. M., Ong, I. M., Denu, J. M., Markley, J. L., Coon, J. J., Colman, R. J., *et al.* (2018) Caloric restriction engages hepatic RNA processing mechanisms in Rhesus monkeys. *Cell Metab.* **27**, 677–688.e675
2. Petersen, M. C., Vatner, D. F., and Shulman, G. I. (2017) Regulation of hepatic glucose metabolism in health and disease. *Nat. Rev. Endocrinol.* **13**, 572–587
3. Haeusler, R. A., Kaestner, K. H., and Accili, D. (2010) FoxOs function synergistically to promote glucose production. *J. Biol. Chem.* **285**, 35245–35248
4. Puigserver, P., Rhee, J., Donovan, J., Walkey, C. J., Yoon, J. C., Oriente, F., Kitamura, Y., Altomonte, J., Dong, H., Accili, D., and Spiegelman, B. M. (2003) Insulin-regulated hepatic gluconeogenesis through FOXO1-PGC-1alpha interaction. *Nature* **423**, 550–555
5. Schmoll, D., Walker, K. S., Alessi, D. R., Grempler, R., Burchell, A., Guo, S., Walther, R., and Unterman, T. G. (2000) Regulation of glucose-6-phosphatase gene expression by protein kinase Balpha and the forkhead transcription factor FKHR. Evidence for insulin response unit-dependent and -independent effects of insulin on promoter activity. *J. Biol. Chem.* **275**, 36324–36333
6. Hall, R. K., Yamasaki, T., Kucera, T., Waltner-Law, M., O'Brien, R., and Granner, D. K. (2000) Regulation of phosphoenolpyruvate carboxykinase and insulin-like growth factor-binding protein-1 gene expression by insulin. The role of winged helix/forkhead proteins. *J. Biol. Chem.* **275**, 30169–30175
7. Kops, G. J., de Ruiter, N. D., De Vries-Smits, A. M., Powell, D. R., Bos, J. L., and Burgering, B. M. (1999) Direct control of the Forkhead transcription factor AFX by protein kinase B. *Nature* **398**, 630–634
8. Nakae, J., Oki, M., and Cao, Y. (2008) The FoxO transcription factors and metabolic regulation. *FEBS Lett.* **582**, 54–67
9. Armoni, M., Harel, C., Karni, S., Chen, H., Bar-Yoseph, F., Ver, M. R., Quon, M. J., and Karnieli, E. (2006) FOXO1 represses peroxisome proliferator-activated receptor-gamma1 and -gamma2 gene promoters in primary adipocytes. A novel paradigm to increase insulin sensitivity. *J. Biol. Chem.* **281**, 19881–19891
10. Qu, S., Altomonte, J., Perdomo, G., He, J., Fan, Y., Kamagate, A., Meseck, M., and Dong, H. H. (2006) Aberrant Forkhead box O1 function is associated with impaired hepatic metabolism. *Endocrinology* **147**, 5641–5652
11. Valenti, L., Rametta, R., Dongiovanni, P., Maggioni, M., Fracanzani, A. L., Zappa, M., Lattuada, E., Roviaro, G., and Fargion, S. (2008) Increased expression and activity of the transcription factor FOXO1 in nonalcoholic steatohepatitis. *Diabetes* **57**, 1355–1362
12. Zhang, K., Li, L., Qi, Y., Zhu, X., Gan, B., DePinho, R. A., Averitt, T., and Guo, S. (2012) Hepatic suppression of Foxo1 and Foxo3 causes hypoglycemia and hyperlipidemia in mice. *Endocrinology* **153**, 631–646
13. Matsumoto, M., Pocai, A., Rossetti, L., Depinho, R. A., and Accili, D. (2007) Impaired regulation of hepatic glucose production in mice lacking the forkhead transcription factor Foxo1 in liver. *Cell Metab.* **6**, 208–216
14. Nakae, J., Biggs, W. H., 3rd, Kitamura, T., Cavenee, W. K., Wright, C. V., Arden, K. C., and Accili, D. (2002) Regulation of insulin action and pancreatic beta-cell function by mutated alleles of the gene encoding forkhead transcription factor Foxo1. *Nat. Genet.* **32**, 245–253
15. Kim, J. J., Li, P., Huntley, J., Chang, J. P., Arden, K. C., and Olefsky, J. M. (2009) FoxO1 haploinsufficiency protects against high-fat diet-induced insulin resistance with enhanced peroxisome proliferator-activated receptor gamma activation in adipose tissue. *Diabetes* **58**, 1275–1282
16. Dong, X. C., Copps, K. D., Guo, S., Li, Y., Kollipara, R., DePinho, R. A., and White, M. F. (2008) Inactivation of hepatic Foxo1 by insulin signaling is required for adaptive nutrient homeostasis and endocrine growth regulation. *Cell Metab.* **8**, 65–76
17. Lu, M., Wan, M., Leavens, K. F., Chu, Q., Monks, B. R., Fernandez, S., Ahima, R. S., Ueki, K., Kahn, C. R., and Birnbaum, M. J. (2012) Insulin regulates liver metabolism *in vivo* in the absence of hepatic Akt and Foxo1. *Nat. Med.* **18**, 388–395
18. Zhang, Y., Wang, Z., Zhao, Y., Zhao, M., Wang, S., Hua, Z., and Zhang, J. (2012) The plasma 5′-AMP acts as a potential upstream regulator of hyperglycemia in type 2 diabetic mice. *Am. J. Physiol. Endocrinol. Metab.* **302**, E325–E333
19. Yang, X., Zhao, Y., Sun, Q., Yang, Y., Gao, Y., Ge, W., Liu, J., Xu, X., Weng, D., Wang, S., and Zhang, J. (2019) Adenine nucleotide-mediated regulation of hepatic PTP1B activity in mouse models of type 2 diabetes. *Diabetologia* **62**, 2106–2117
20. Antonioli, L., Blandizzi, C., Csoka, B., Pacher, P., and Hasko, G. (2015) Adenosine signalling in diabetes mellitus–pathophysiology and therapeutic considerations. *Nat. Rev. Endocrinol.* **11**, 228–241
21. Wu, L. F., Li, G. P., Feng, J. L., and Pu, Z. J. (2006) Molecular mechanisms of adenosine-induced apoptosis in human HepG2 cells. *Acta Pharmacol. Sin.* **27**, 477–484
22. Lombardini, J. B., Coulter, A. W., and Talalay, P. (1970) Analogues of methionine as substrates and inhibitors of the methionine adenosyltransferase reaction. Deductions concerning the conformation of methionine. *Mol. Pharmacol.* **6**, 481–499
23. Moore, L. D., Le, T., and Fan, G. (2013) DNA methylation and its basic function. *Neuropsychopharmacology* **38**, 23–38
24. Mozzetta, C., Boyarchuk, E., Pontis, J., and Ait-Si-Ali, S. (2015) Sound of silence: The properties and functions of repressive Lys methyltransferases. *Nat. Rev. Mol. Cell Biol.* **16**, 499–513
25. Kitamura, T. (2013) The role of FOXO1 in β-cell failure and type 2 diabetes mellitus. *Nat. Rev. Endocrinol.* **9**, 615–623
26. Hawkins, M., Tonelli, J., Kishore, P., Stein, D., Ragucci, E., Gitig, A., and Reddy, K. (2003) Contribution of elevated free fatty acid levels to the lack of glucose effectiveness in type 2 diabetes. *Diabetes* **52**, 2748–2758
27. Yang, X., Zhao, Y., Sun, Q., Yang, Y. X., Gao, Y., Ge, W. H., Liu, J. H., Xu, X., and Zhang, J. F. (2019) An intermediary role of adenine nucleotides on free fatty acids-induced hyperglycemia in obese mice. *Front. Endocrinol.* **10**, 497
28. Resta, R., Yamashita, Y., and Thompson, L. F. (1998) Ecto-enzyme and signaling functions of lymphocyte CD73. *Immunol. Rev.* **161**, 95–109
29. Chen, J. F., Eltzschig, H. K., and Fredholm, B. B. (2013) Adenosine receptors as drug targets–what are the challenges? *Nat. Rev. Drug Discov.* **12**, 265–286
30. Friedman, B., Corciulo, C., Castro, C. M., and Cronstein, B. N. (2021) Adenosine A2A receptor signaling promotes FoxO associated autophagy in chondrocytes. *Sci. Rep.* **11**, 968
31. Zhan, Y., Wang, Z., Yang, P., Wang, T., Xia, L., Zhou, M., Wang, Y., Wang, S., Hua, Z., and Zhang, J. (2014) Adenosine 5′-monophosphate ameliorates D-galactosamine/lipopolysaccharide-induced liver injury through an adenosine receptor-independent mechanism in mice. *Cell Death Dis.* **5**, e985
32. Pastor-Anglada, M., and Pérez-Torras, S. (2018) Who is Who in adenosine transport. *Front. Pharmacol.* **9**, 627
33. Xia, L., Ma, S., Zhang, Y., Wang, T., Zhou, M., Wang, Z., and Zhang, J. (2015) Daily variation in global and local DNA methylation in mouse livers. *PLoS One* **10**, e0118101
34. Poirier, L. A., Brown, A. T., Fink, L. M., Wise, C. K., Randolph, C. J., Delongchamp, R. R., and Fonseca, V. A. (2001) Blood S-adenosylmethionine concentrations and lymphocyte methylenetetrahydrofolate reductase activity in diabetes mellitus and diabetic nephropathy. *Metab. Clin. Exp.* **50**, 1014–1018
35. Ratnam, S., Wijekoon, E. P., Hall, B., Garrow, T. A., Brosnan, M. E., and Brosnan, J. T. (2006) Effects of diabetes and insulin on betaine-

homocysteine S-methyltransferase expression in rat liver. *Am. J. Physiol. Endocrinol. Metab.* **290**, E933–939
36. Becker, A., Henry, R. M., Kostense, P. J., Jakobs, C., Teerlink, T., Zweegman, S., Dekker, J. M., Nijpels, G., Heine, R. J., Bouter, L. M., Smulders, Y. M., and Stehouwer, C. D. (2003) Plasma homocysteine and S-adenosylmethionine in erythrocytes as determinants of carotid intima-media thickness: Different effects in diabetic and non-diabetic individuals. *Hoorn Study Atheroscler.* **169**, 323–330
37. Cuyàs, E., Fernández-Arroyo, S., Verdura, S., García, R., Stursa, J., Werner, L., Blanco-González, E., Montes-Bayón, M., Joven, J., Viollet, B., Neuzil, J., and Menendez, J. A. (2018) Metformin regulates global DNA methylation via mitochondrial one-carbon metabolism. *Oncogene* **37**, 963–970
38. Greer, E. L., and Shi, Y. (2012) Histone methylation: A dynamic mark in health, disease and inheritance. *Nat. Rev. Genet.* **13**, 343–357
39. Stewart, M. D., Li, J., and Wong, J. (2005) Relationship between histone H3 lysine 9 methylation, transcription repression, and heterochromatin protein 1 recruitment. *Mol. Cell. Biol.* **25**, 2525–2538
40. Xia, L., Wang, Z. Q., Zhang, Y., Yang, X., Zhan, Y. B., Cheng, R., Wang, S. M., and Zhang, J. F. (2015) Reciprocal regulation of insulin and plasma 5 '-AMP in glucose homeostasis in mice. *J. Endocrinol.* **224**, 225–234
41. Chen, J., Zhou, X., Wu, W., Wang, X., and Wang, Y. (2015) FTO-dependent function of N6-methyladenosine is involved in the hepatoprotective effects of betaine on adolescent mice. *J. Physiol. Biochem.* **71**, 405–413
42. Lee, C. C., Surtees, R., and Duchen, L. W. (1992) Distal motor axonopathy and central nervous system myelin vacuolation caused by cycloleucine, an inhibitor of methionine adenosyltransferase. *Brain* **115**(Pt 3), 935–955
43. Radović, B., Vujić, N., Leopold, C., Schlager, S., Goeritzer, M., Patankar, J. V., Korbelius, M., Kolb, D., Reindl, J., Wegscheider, M., Tomin, T., Birner-Gruenberger, R., Schittmayer, M., Groschner, L., Magnes, C., *et al.* (2016) Lysosomal acid lipase regulates VLDL synthesis and insulin sensitivity in mice. *Diabetologia* **59**, 1743–1752
44. Yang, Y., Tarabra, E., Yang, G. S., Vaitheesvaran, B., Palacios, G., Kurland, I. J., Pessin, J. E., and Bastie, C. C. (2013) Alteration of de novo glucose production contributes to fasting hypoglycaemia in Fyn deficient mice. *PLoS One* **8**, e81866
45. Clark, S. J., Harrison, J., Paul, C. L., and Frommer, M. (1994) High sensitivity mapping of methylated cytosines. *Nucleic Acids Res.* **22**, 2990–2997
46. Knudsen, T. B., Winters, R. S., Otey, S. K., Blackburn, M. R., Airhart, M. J., Church, J. K., and Skalko, R. G. (1992) Effects of (R)-deoxycoformycin (pentostatin) on intrauterine nucleoside catabolism and embryo viability in the pregnant mouse. *Teratology* **45**, 91–103
47. Braunstein, M., Rose, A. B., Holmes, S. G., Allis, C. D., and Broach, J. R. (1993) Transcriptional silencing in yeast is associated with reduced nucleosome acetylation. *Genes Dev.* **7**, 592–604
48. Spencer, V. A., Sun, J. M., Li, L., and Davie, J. R. (2003) Chromatin immunoprecipitation: A tool for studying histone acetylation and transcription factor binding. *Methods* **31**, 67–75
49. Zhou, Y. F., Wu, X. M., Zhou, G., Mu, M. D., Zhang, F. L., Li, F. M., Qian, C., Du, F., Yung, W. H., Qian, Z. M., and Ke, Y. (2018) Cystathionine β-synthase is required for body iron homeostasis. *Hepatology* **67**, 21–35
50. Yadav, H., Devalaraja, S., Chung, S. T., and Rane, S. G. (2017) TGF-beta1/Smad3 pathway targets PP2A-AMPK-FoxO1 signaling to regulate hepatic gluconeogenesis. *J. Biol. Chem.* **292**, 3420–3432